# Supporting Information

## Nakagawa et al. 10.1073/pnas.1322731111

### SI Materials and Methods

**Reagents.** The following antibodies were used in these experiments: anti–E-cadherin, anti–phospho-ERK, anti-vimentin, and anti-CD44 for Western blotting (Cell Signaling); anti-CD44 for immunohistochemistry and anti-CD44v6 (AbD Serotec); anti-Sox9 and anti-K19 (Santa Cruz Biotechnology); anti–N-cadherin (Millipore); anti-actin and anti-tubulin (Sigma); anti-EpCAM (Abcam); anti–α-smooth muscle actin (Dako); anti-CD45 (eBioscience); anti-F4/80 (Caltag); anti-Ki67 (GeneTex); anti–α-fetoprotein (AFP) (Biocare Medical); anti–β-catenin (GeneTex and BD Transduction Laboratories); and anti-Snail (Novus Biologicals). Recombinant human TNF-α, hepatocyte growth factor, and TGF-β were purchased from R&D Systems.

**Immunoblotting.** Whole-liver protein homogenates were subjected to SDS/PAGE and transferred to a polyvinylidene membrane (Amersham Biosciences). The membrane was probed with primary antibodies and then incubated with the secondary antibody. Immunocomplexes were detected using the ECL System (Amersham Biosciences). Phospho-RTK (receptor tyrosine kinase) array was performed using the Proteome Profiler Mouse Phospho-RTK Array Kit (R&D Systems) according to the manufacturer's protocol.

**RNA Extraction and Real-Time PCR.** RNA was extracted from liver tissue using ISOGEN (Nippon Gene). First-strand cDNA was synthesized using SuperScript 2 (Invitrogen Life Technologies), and the relative amount of each mRNA was quantified by real-time PCR and normalized against GAPDH mRNA expression. Primer sequences are available upon request.

**Histology.** Livers were fixed in 10% (vol/vol) neutral-buffered formalin or 4% (wt/vol) paraformaldehyde, embedded in paraffin, sectioned, and stained with hematoxylin and eosin (H&E) or Sirius red, and processed for immunohistochemistry. In the case of immunostaining of E-cadherin, perfusion fixation was performed with 4% paraformaldehyde. For frozen block preparation, liver tissue was embedded in Tissue-Tek OCT compound (Sakura Finetek). For immunohistochemistry, fixed and paraffin-embedded liver sections were deparaffinized and incubated in citrate buffer at 95 °C for 40 min for antigen retrieval, and then incubated overnight at 4 °C with the primary antibodies. Biotinylated secondary antibodies (Pharmingen) were added and incubated for 20 min at room temperature. Streptavidin-horseradish peroxidase (Pharmingen) was added, and after 30 min the sections were developed with 3,3′-diaminobenzidine substrate and counterstained with hematoxylin. Quantification of the stained area was performed with ImageJ software (National Institutes of Health). Frozen slides were incubated with primary antibodies, followed by secondary antibodies labeled with Alexa 488 or 594 (Molecular Probes).

The expression of E-cadherin in human primary sclerosing cholangitis (PSC) samples was analyzed using liver explants and biopsy samples containing medium or large bile ducts. Adjacent nontumor tissue of metastatic liver cancer was used as a normal control. Liver explants were obtained through the Cooperative Human Tissue Network, and biopsy samples for the diagnosis of PSC were obtained at the University of Tokyo with approval of the medical ethics committee of the University of Tokyo and with informed consent.

The tissue array was purchased from US Biomax and contained 60 paired human hepatocellular carcinoma (HCC) and nontumor tissues. When the number of E-cadherin–positive cells was <25% of the tumor cell population, the sample was defined as E-cadherin–negative. CD44 and vimentin expression in the tumors were scored semiquantitatively based on a scale staining pattern of 0–3 (0, all tumor cells are negative; 1, ≤25%; 2, 25–50%; 3, >50% of the tumor cell population is positive for CD44 or vimentin).

TUNEL staining was performed using an ApoAlert DNA Fragmentation Assay Kit (Clontech).

**Electron Microscopy.** Livers were fixed with 2% glutaraldehyde/0.1 M phosphate buffer (pH 7.4) and then postfixed with 1% osmium tetroxide/0.1 M phosphate buffer (pH 7.4). Fixed samples were embedded in epoxy resin. Ultrathin sections were counterstained with uranyl acetate and observed with a JEOL 1200 EXII electron microscope.

**Immunofluorescence Microscopy for Fluorescent-Labeled Bile Acid.** Fluorescent-labeled bile acid was kindly provided by Alan Hofmann (University of California, San Diego), and 100 μL of a 2 mM solution was injected into the tail veins of 2-mo-old $CDH1^{F/F}$ and $CDH1^{\Delta L}$ mice. Fifteen minutes after injection, the mice were killed and the removed livers were embedded in OCT compound. Sections from frozen tissues were visualized by fluorescence microscopy.

**Adenovirus- and Tamoxifen-Induced Gene Recombination in Vivo.** Recombinant adenovirus expressing Cre-recombinase and control empty adenovirus vector were diluted in PBS and i.v. injected into mice ($1 \times 10^9$ plaque-forming units per mouse). Tamoxifen (TAM) was dissolved in corn oil and intraperitoneally injected (4 mg TAM per mouse).

**Microarray Analysis.** Microarray analysis was performed using SurePrint G3 Mouse Gene Expression 8 × 60K arrays (Agilent Technologies) according to the manufacturer's protocol. Data were preprocessed using Agilent GeneSpring GX11.

**Diethylnitrosamine-Induced Hepatocellular Carcinoma.** Diethylnitrosamine (DEN) (Sigma) was dissolved in PBS and injected intraperitoneally into mice (25 mg/kg) on postnatal day 14. Mice were killed after 8 mo, and their livers were removed and examined for visible tumors.

**Cell Culture, Transfections, and RNA Interference.** HuH7, Alexander, HLF, HepG2, and SK-Hep1 cell lines as well as a human normal hepatocyte cell line were cultured in Dulbecco's modified Eagle medium with 10% FBS. Hep3B cells were cultured in minimum essential medium (MEM) with 2 mM L-glutamine, 0.15% sodium bicarbonate, 0.1 mM nonessential amino acid solution, 1 mM sodium pyruvate, and 10% FBS. JHH4 cells were cultured in MEMa with 10% FBS. Li7 cells were cultured in RPMI-1640 with 10% FBS. Mouse primary hepatocytes were isolated by the collagenase perfusion method and then cultured in William's E medium with 10% FBS on collagen-coated plates.

A small interfering RNA (siRNA) construct was obtained with siGENOME SMARTpool reagents (Dharmacon), and siRNA transfections were performed using RNAiMAX (Invitrogen). pCMV3 myc-tagged RasG12V plasmid was transfected into normal human hepatocyte cell lines using X-tremeGENE HP DNA Transfection Reagent (Roche). Subcellular protein fractionation was performed using the ProteoExtract Subcellular Proteome Extraction Kit (Calbiochem).

**Invasion Assay.** An invasion assay was performed using a BD BioCoat Matrigel invasion chamber containing 8.0-μm pore size polyethylene terephthalate membrane inserts in a 24-well format, according to the manufacturer's protocol. Briefly, 5 d after transfection with E-cadherin or control siRNA, $1 \times 10^4$ cells were added to the upper chambers in serum-free culture media. The lower chamber

contained 10% FBS. After 24 h, cells on the upper surface of each membrane were removed with cotton swabs, and those that successfully migrated to the lower surface were stained with the Diff-Quick Kit (Sysmex, Japan) and counted. Data are expressed as the percent invasion through the Matrigel and membrane relative to the number of cells migrating through the control membrane.

**Mice.** $APC^{F/F}$ mice have been described previously (1).

**Statistical Analyses.** Statistical analyses were performed using the Student *t* test or one-way analysis of variance followed by the Tukey–Kramer test for multiple comparisons. A $P$ value $<0.05$ indicated statistical significance.

1. Grivennikov SI, et al. (2012) Adenoma-linked barrier defects and microbial products drive IL-23/IL-17-mediated tumour growth. *Nature* 491(7423):254–258.

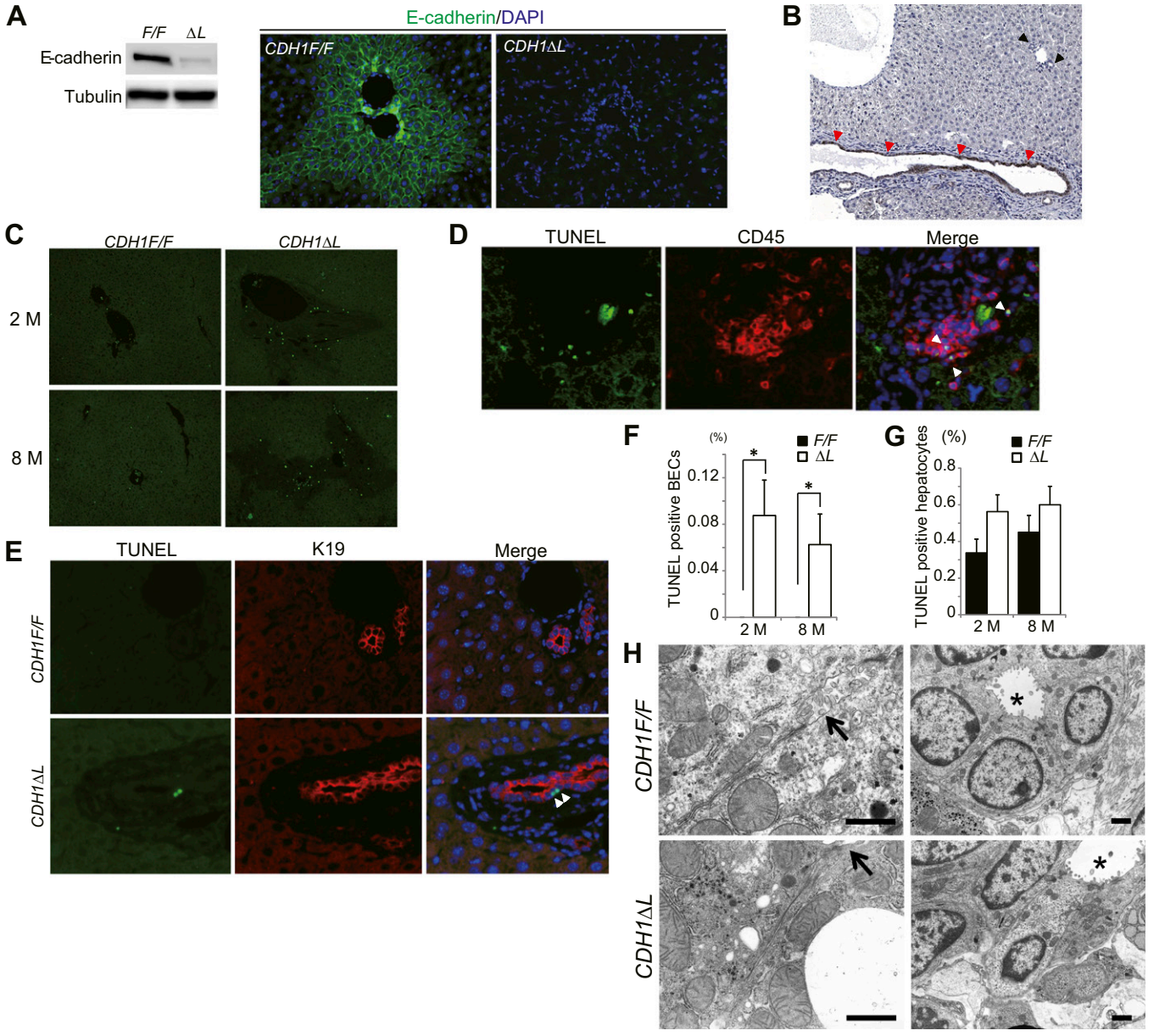


**Fig. S1.** Characterization of $CDH1^{\Delta L}$ mouse livers. (*A*) Analysis of E-cadherin expression by Western blotting of total liver protein and immunofluorescence (IF) staining of liver sections obtained from 1-mo-old $CDH1^{F/F}$ and $CDH1^{\Delta L}$ mice (×200). Nuclei were labeled with DAPI (blue). (*B*) Immunohistochemistry (IHC) analysis of E-cadherin expression in 1-mo-old $CDH1^{\Delta L}$ mouse liver. Expression of E-cadherin was absent in the interlobular bile duct (black arrowheads) but not in the large bile duct near the common bile duct (red arrowheads) (×200). (*C*) Representative TUNEL-stained sections in 2- and 8-mo-old $CDH1^{F/F}$ and $CDH1^{\Delta L}$ mouse livers (×200). (*D*) Double IF staining of TUNEL (green) and pan-leukocyte marker CD45 (red) in the periportal area of 2-mo-old $CDH1^{\Delta L}$ mouse liver (×400). Arrowheads indicate TUNEL-CD45 double-positive cells. (*E*) Double IF staining of TUNEL (green) and biliary epithelial cell (BEC) marker K19 (red) in 2-mo-old $CDH1^{F/F}$ and $CDH1^{\Delta L}$ mouse livers (×400). Arrowheads indicate TUNEL-K19 double-positive cells. (*F* and *G*) Frequencies of TUNEL-positive duct cells (*F*) and hepatocytes (*G*) in 2- and 8-mo-old $CDH1^{F/F}$ and $CDH1^{\Delta L}$ mouse livers. Data are expressed as means ± SEM ($n = 8$ per group; $^*P < 0.05$.). (*H*) Electron microscopic images of junction complexes in hepatocytes (*Left*) and bile duct cells (*Right*) in 2-mo-old $CDH1^{F/F}$ and $CDH1^{\Delta L}$ mice. (Scale bars, 1 μm.) Arrows and asterisks indicate bile canaliculi and bile duct lumens, respectively.

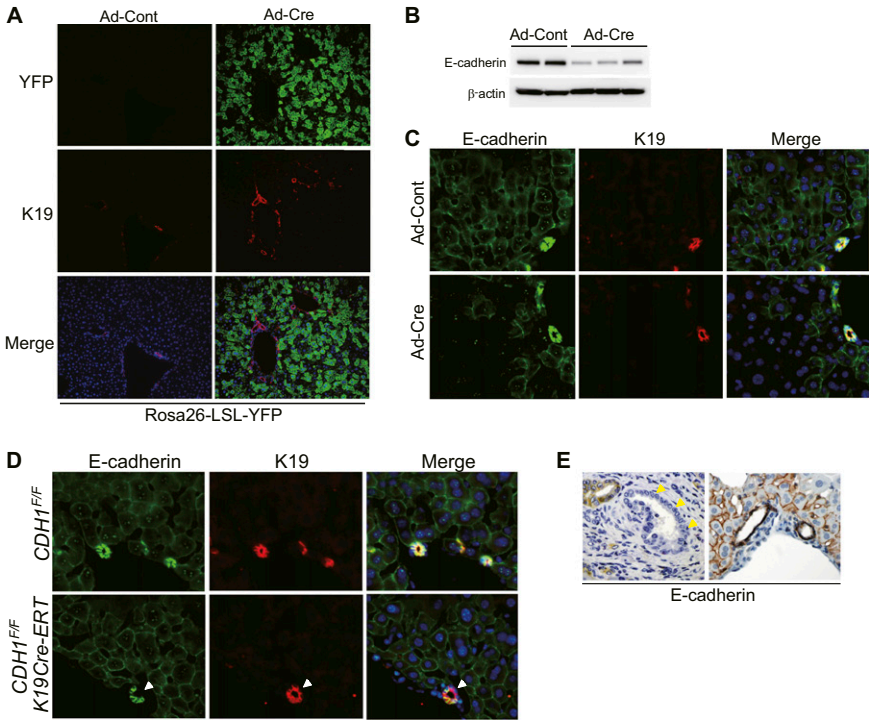


**Fig. S2.** Separated analysis of the role of E-cadherin in hepatocytes and BECs to maintain liver homeostasis. (*A*) Ad-Cre or Ad-Cont (control adenovirus) was i.v. injected into Rosa26-lox-stop-lox-YFP mice, and 1 wk later, hepatocyte-specific Cre-loxP recombination was confirmed by double IF staining of YFP (green) and K19 (red) (×200). (*B* and *C*) Analysis of E-cadherin expression in *CDH1*$^{F/F}$ mouse liver at 8 wk after Ad-Cre or Ad-Cont injection. Western blotting of total liver protein shows significant reduction of E-cadherin protein in Ad-Cre–injected mice compared with Ad-Cont–injected mice (*B*). Double IF staining of E-cadherin (green) and K19 (red) shows that expression of E-cadherin in hepatocytes was frequently deleted, whereas that in BECs was well-preserved (×400) (*C*). (*D*) TAM was intraperitoneally injected into *CDH1*$^{F/F}$ and *CDH1*$^{F/F}$/*K19*$^{CreERT}$ mice, and 1 wk later, BEC-specific deletion of E-cadherin was confirmed by double IF staining of E-cadherin (green) and K19 (red) (×400). Arrowheads indicate E-cadherin–deleted K19-positive BECs. (*E*) IHC analysis of E-cadherin expression in *CDH1*$^{F/F}$/*K19*$^{CreERT}$ mouse liver at 8 wk after TAM injection (×400). (*Left*) Efficient deletion of E-cadherin in BECs with strong periductal inflammation. (*Right*) Inefficient deletion without inflammation. Arrowheads indicate efficiently E-cadherin–deleted bile duct.

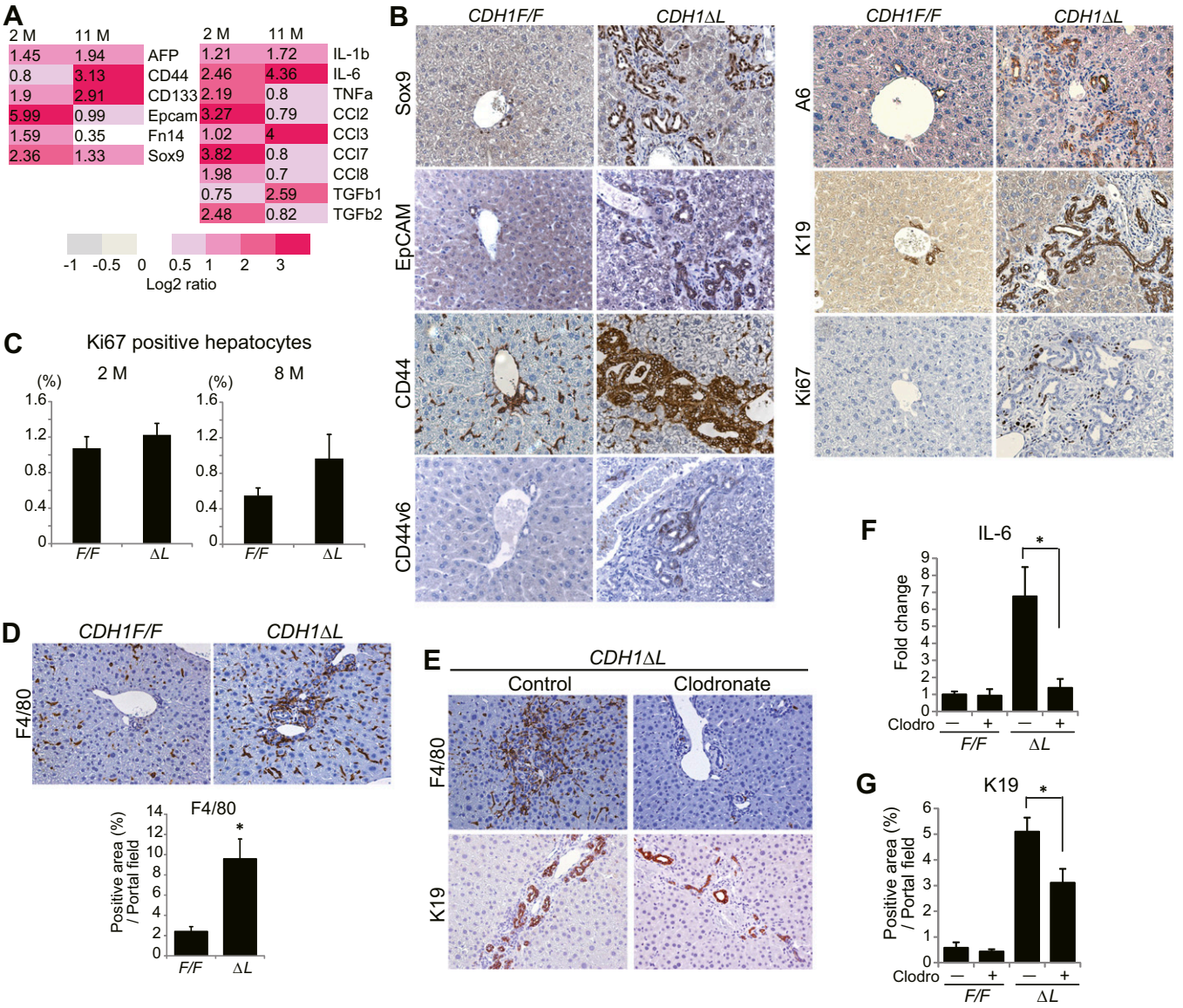


**Fig. S3.** Ductular reaction in *CDH1*$^{\Delta L}$ mice. (*A*) cDNA microarray analysis of whole-liver samples from *CDH1*$^{F/F}$ and *CDH1*$^{\Delta L}$ mice at 2 and 11 mo of age. Expression of stem cell markers (*Left*) and inflammatory cytokines and chemokines (*Right*) is up-regulated in *CDH1*$^{\Delta L}$ mice compared with *CDH1*$^{F/F}$ mice. Representative genes are shown and data are expressed as log2 ratio. (*B*) IHC analysis of the indicated stem cell and proliferation markers in 8-mo-old *CDH1*$^{F/F}$ and *CDH1*$^{\Delta L}$ mice (×400). (*C*) Frequencies of Ki67-positive hepatocytes in 2- and 8-mo-old *CDH1*$^{F/F}$ and *CDH1*$^{\Delta L}$ mouse livers. Data are expressed as means ± SEM ($n$ = 4–6 per group). (*D*) IHC analysis of F4/80 in 8-mo-old *CDH1*$^{F/F}$ and *CDH1*$^{\Delta L}$ mice (×200). The bar graph shows F4/80-positive areas. Data are expressed as means ± SD ($n$ = 5 per group; *$P < 0.05$). (*E–G*) Effect of macrophage depletion on the ductular reaction. Two-month-old *CDH1*$^{F/F}$ and *CDH1*$^{\Delta L}$ mice were i.v. injected with 100 μL liposomal clodronate or PBS liposome (control) four times every 4 d (days 1, 5, 9, and 13) ($n$ = 3–4 per group). The mice were killed 4 d after the final injection. IHC analysis of the indicated proteins in liposomal clodronate or control-injected *CDH1*$^{\Delta L}$ mice (×200) (*E*). The relative level of IL-6 mRNA was determined by real-time PCR (*F*). K19-positive areas were quantified (*G*). Data are expressed as means ± SD; *$P < 0.05$.

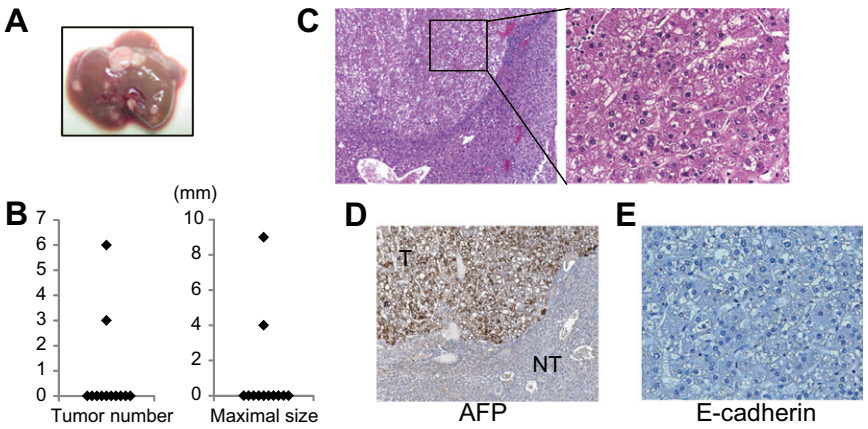


**Fig. S4.** Some *CDH1*$^{\Delta L}$ mice spontaneously develop liver tumors. (*A*) Representative image of a tumor-bearing liver in an 11-mo-old *CDH1*$^{\Delta L}$ mouse. (*B*) Graphs show tumor number and maximal tumor size in 11-mo-old *CDH1*$^{\Delta L}$ mice ($n = 12$). (*C*) H&E staining of a liver tumor in a *CDH1*$^{\Delta L}$ mouse (*Left*, ×100; *Right*, ×400). (*D* and *E*) IHC analysis of AFP and E-cadherin expression in tumor tissue (*D*, ×100; *E*, ×400). NT, nontumor; T, tumor.

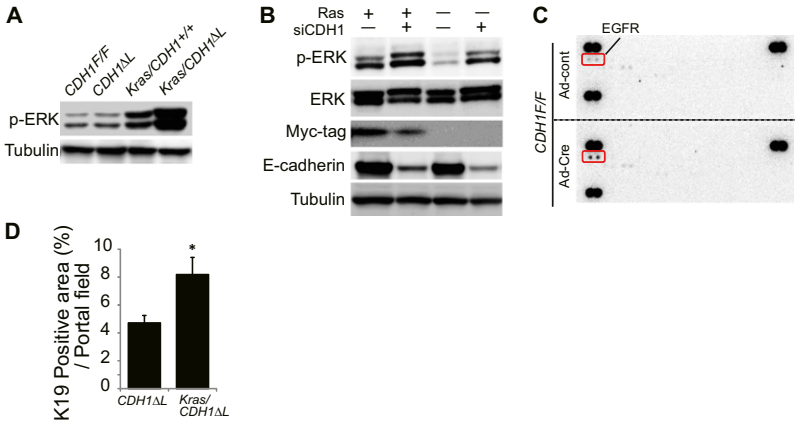


**Fig. S5.** Cooperative activation of ERK by active Ras and loss of E-cadherin. (*A*) Western blot evaluation of ERK phosphorylation in nontumor tissues of 8-mo-old mouse livers. (*B*) Normal immortalized human hepatocytes were transfected with myc-tagged active Ras (G12V) and siRNA targeted to E-cadherin. The indicated proteins were assessed by Western blotting. (*C*) Primary hepatocytes isolated from *CDH1*$^{F/F}$ mice were infected with Ad-Cont or Ad-Cre and, 48 h afterward, RTK phosphorylation was assessed by phospho-RTK array. (*D*) Quantification of a K19-positive area in 8-mo-old *CDH1*$^{\Delta L}$ and *Kras/CDH1*$^{\Delta L}$ mouse livers (related to Fig. 3*G*). The bar graph shows K19-positive areas. Data are expressed as means ± SD ($n = 5$ per group; $^*P < 0.05$).

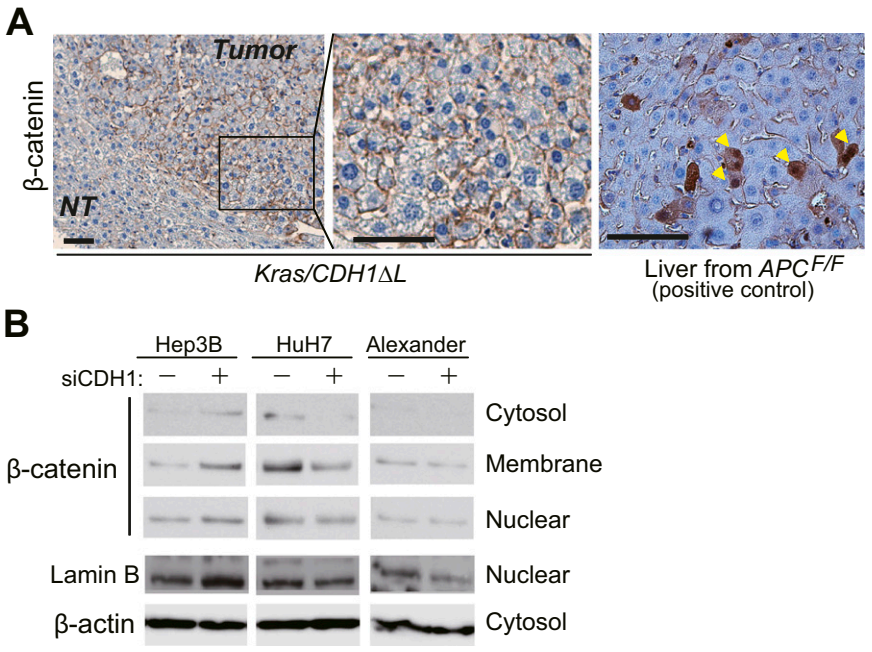


**Fig. S6.** Effect of E-cadherin loss on β-catenin activation. (*A*) Immunohistochemical analysis of β-catenin expression in tumor and nontumor areas of *Kras/CDH1*$^{\Delta L}$ mouse liver (*Left* and *Center*). (Scale bars, 50 μm.) Liver obtained from an APC flox/flox (*APC*$^{F/F}$) mouse, in which β-catenin/TCF signaling is activated due to reduced APC protein, was used as a positive control (*Right*). Arrowheads indicate hepatocytes positive for nuclear β-catenin. (*B*) Analysis of β-catenin expression in fractionated Hep3B, HuH7, and Alexander cells 6 d after transfection with E-cadherin siRNA or control siRNA. Proteins from the cytosolic, membrane, and nuclear fractions were separated, and β-catenin expression levels were assessed by Western blotting.

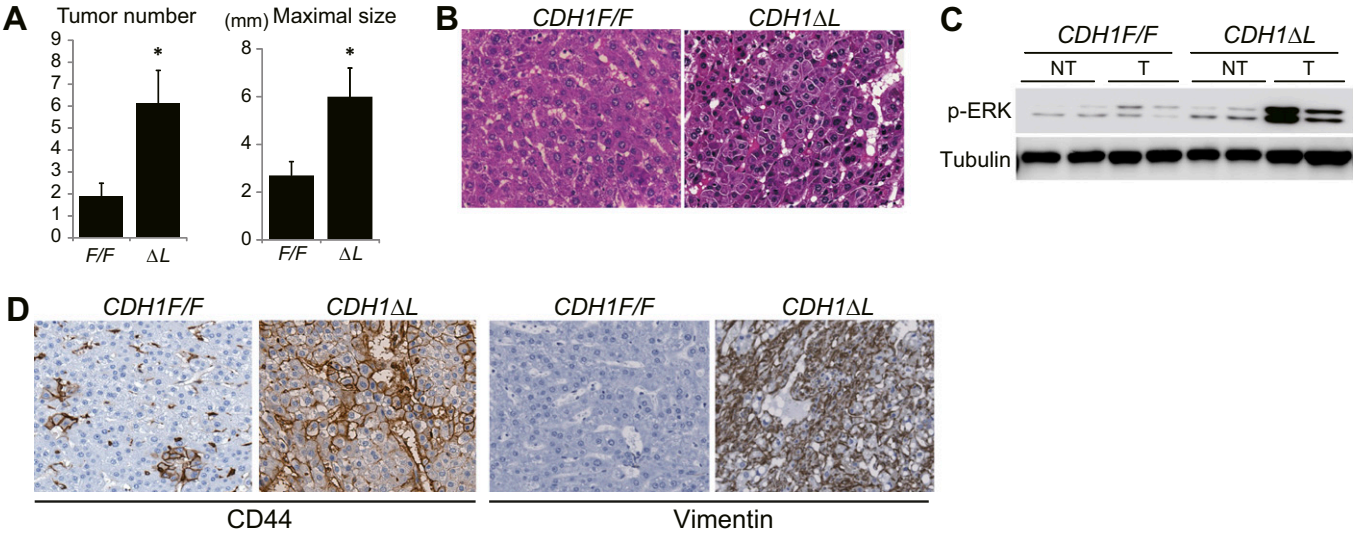


**Fig. S7.** Loss of E-cadherin promotes DEN-induced HCC. (*A*) *CDH1*$^{F/F}$ ($n = 11$) and *CDH1*$^{\Delta L}$ ($n = 16$) mice were injected with 25 mg/kg DEN on postnatal day 14. After 8 mo, tumor number and tumor size were determined. Data are expressed as the means ± SEM, $^{*}P < 0.05$, compared with *CDH1*$^{F/F}$ mice. (*B*) Representative H&E staining of tumors from DEN-treated *CDH1*$^{F/F}$ and *CDH1*$^{\Delta L}$ mice (×400). (*C*) Western blotting of ERK phosphorylation in NT and T tissues from *CDH1*$^{F/F}$ and *CDH1*$^{\Delta L}$ mice. (*D*) Expression of CD44 and vimentin in tumor tissues from *CDH1*$^{F/F}$ and *CDH1*$^{\Delta L}$ mice was assessed by IHC (×400).

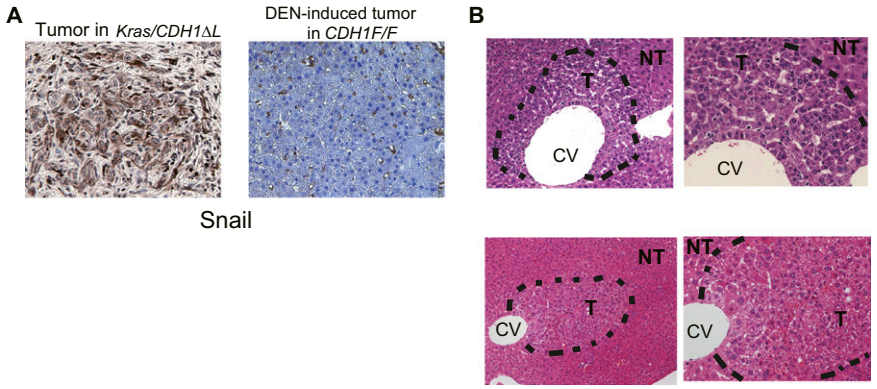


**Fig. S8.** Characteristics of *Kras/CDH1*$^{\Delta L}$ tumors. (*A*) IHC analysis of Snail in *Kras/CDH1*$^{\Delta L}$ tumors (*Left*, ×400). Tumor cells undergoing epithelial–mesenchymal transition (EMT) strongly expressed Snail. A DEN-induced tumor in *CDH1*$^{F/F}$ mice was used as a negative control (*Right*, ×400). (*B*) Some tumors in *Kras/CDH1*$^{\Delta L}$ mice arise from zone 3. H&E staining images of two representative tumors arising from zone 3 in *Kras/CDH1*$^{\Delta L}$ mice (*Left*, ×200; *Right*, ×400). These tumors are adjacent to the central vein (CV) , which is distant from the portal area.

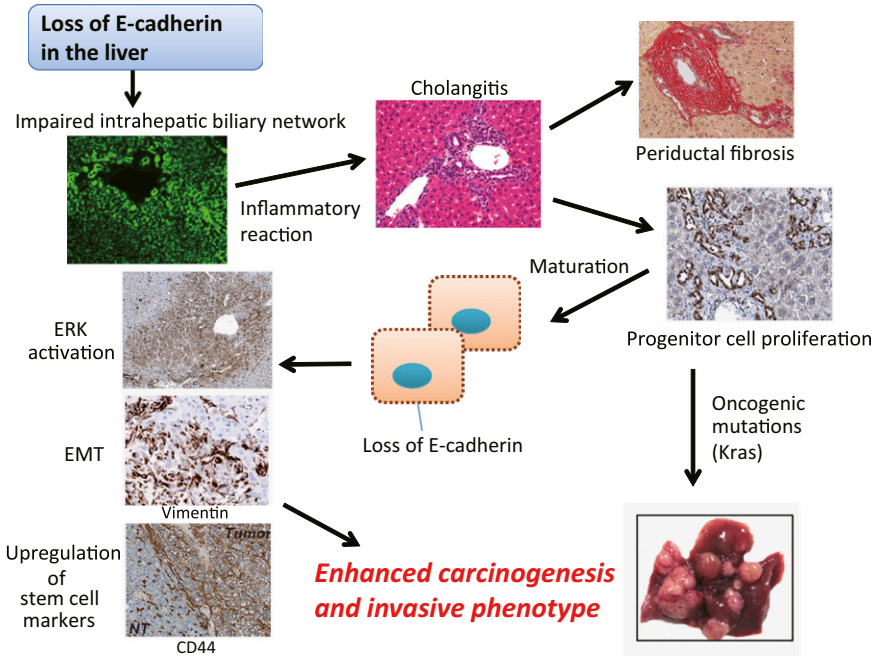


**Fig. S9.** Proposed mechanism by which loss of E-cadherin induces sclerosing cholangitis and promotes carcinogenesis. Loss of E-cadherin in the liver, especially in BECs, causes impairment of the intrahepatic biliary network and subsequent inflammatory reactions that lead to progenitor cell proliferation and periductal fibrosis. In some cases, these progenitor cells may develop directly into tumors through oncogenic mutations. In mature hepatocytes, loss of E-cadherin leads to ERK activation, EMT induction, and up-regulation of stem cell markers, which eventually results in enhanced carcinogenesis and an invasive phenotype.